

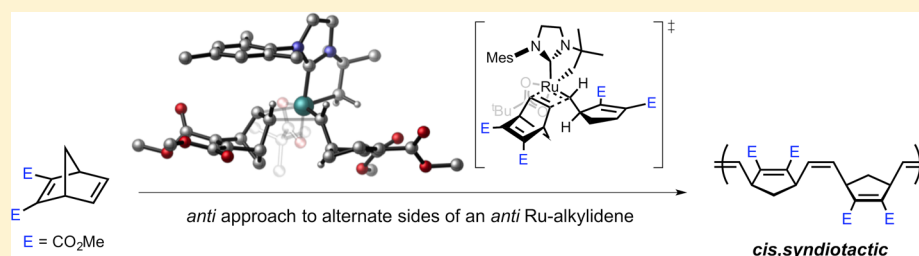
Probing Stereoselectivity in Ring-Opening Metathesis Polymerization Mediated by Cyclometalated Ruthenium-Based Catalysts: A Combined Experimental and Computational Study

L. E. Rosebrugh,[†] T. S. Ahmed,[†] V. M. Marx,[†] J. Hartung,[†] P. Liu,[‡] J. G. López,[‡] K. N. Houk,^{*,‡} and R. H. Grubbs^{*,†}

[†]Arnold and Mabel Beckman Laboratory of Chemical Synthesis, Division of Chemistry and Chemical Engineering, California Institute of Technology, Pasadena, California 91125, United States

[‡]Department of Chemistry and Biochemistry, University of California, Los Angeles, California 90095, United States

S Supporting Information



ABSTRACT: The microstructures of polymers produced by ring-opening metathesis polymerization (ROMP) with cyclometalated Ru-carbene metathesis catalysts were investigated. A strong bias for a *cis,syndiotactic* microstructure with minimal head-to-tail bias was observed. In instances where *trans* errors were introduced, it was determined that these regions were also syndiotactic. Furthermore, hypothetical reaction intermediates and transition structures were analyzed computationally. Combined experimental and computational data support a reaction mechanism in which *cis,syndio*-selectivity is a result of stereogenic metal control, while microstructural errors are predominantly due to alkylidene isomerization via rotation about the Ru=C double bond.

INTRODUCTION

The physical and mechanical properties of polymers formed in ring-opening metathesis polymerization (ROMP) reactions of mono- and polycyclic olefins are strongly related to the degree of order in the polymer microstructures.¹ With respect to norbornene- and norbornadiene-derived ROMP polymers in particular, these microstructures include *cis* or *trans* double bonds; isotactic (*m*) or syndiotactic (*r*) dyads; and, in the case of polymers derived from unsymmetrically substituted monomers, head–tail (HT) dyads or head–head (HH) and tail–tail (TT) dyads (Figure 1).² Precise control of these primary structural elements is fundamental to preparing polymers with well-defined properties.

Significant microstructural control of norbornene- and norbornadiene-based polymers was first achieved using classical, metal-salt type initiators (e.g., RuCl₃, ReCl₅, and OsCl₃), in which selectivity is usually a result of chain-end control.² However, because this type of control results from an influence of the polymer chain on the propagation step, whether through steric crowding or the coordination of recently formed double bonds to the metal center, the stereoselectivity of these systems can vary dramatically depending on the type of monomer and/or reaction conditions employed. As a result, examples of ROMP polymers comprised

predominantly of a single structure produced by these systems are rare.

More recently, the development of molybdenum- and tungsten-based initiators with discrete ligand environments and mechanisms of action has led to the preparation of an increasing number of ROMP polymers with singular microstructures.^{3–6} Fully *cis,isotactic* polymers can be produced from a range of norbornene and norbornadiene-based monomers using W and Mo biphenolate and binaphtholate initiators, which operate through enantiomorphic site control, a primarily steric directing effect derived from the chirality of the biphenolate or binaphtholate ligand.⁴ Additionally, pure *cis,syndiotactic* microstructures are accessible through the use of MAP (monoaryloxy pyrrolide) alkylidene complexes as a result of stereogenic metal control, arising from the inversion of the absolute configuration of the metal center that occurs with each forward metathesis step.⁵ Finally, a few examples of predominantly *trans,syndiotactic* and *trans,isotactic* polymers have been prepared with certain Mo initiators as a consequence of chain-end control and a “turnstile-like” nonmetathesis-based polytopal rearrangement, respectively.^{4b,5c,6}

Received: November 24, 2015

Published: January 4, 2016

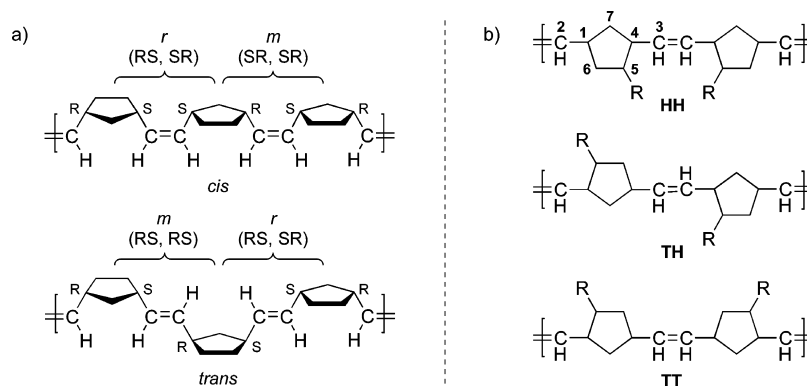


Figure 1. (a) Structural possibilities of norbornene-derived ROMP polymers. (b) Head–head (HH), head–tail (HT), and tail–tail (TT) dyads resulting from polymerization of unsymmetrically substituted norbornenes.

In contrast, only limited control of *cis/trans* content and tacticity has been realized with discrete ruthenium alkylidenes; much like the classical initiators, this stereochemical control is generally dependent on the use of specialized monomers or reaction conditions.⁷ A prevailing theory for the overall lack of stereoselectivity in these systems is that the low calculated barriers of rotation for Ru alkylidenes preclude steric enforcement of polymer tacticities.^{3a,5b,8} Despite this purported limitation, however, we recently reported the generation of highly *cis*, highly syndiotactic ROMP polymers by *N*-^tBu-cyclometalated catalyst **1**, marking the first time a norbornene-based polymer with >95% a single structure had been produced by a ruthenium alkylidene complex (Figure 2).⁹ Catalyst **2**,

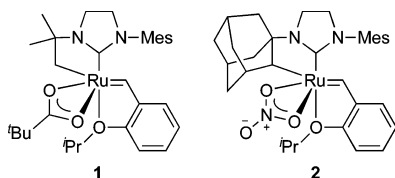


Figure 2. Cyclometalated catalysts **1** and **2** (Mes = 2,4,6-trimethylphenyl).

containing a cyclometalated *N*-adamantyl-*N*-mesityl *N*-heterocyclic carbene (NHC) ligand, has also been shown to yield highly *cis* ROMP polymers, although these polymers were originally thought to be atactic.¹⁰

Because the stereochemical information contained in any given ROMP polymer represents a chronological “road map” of every catalytic cycle that took place over the course of the polymerization, careful microstructural analysis of the dyads and triads in a ROMP polymer can shed light on the exact nature of the propagation transition state(s). ROMP, therefore, presents a powerful tool in which to gain additional insight into the mode-of-action of cyclometalated ruthenium catalysts in *cis*-selective metathesis transformations. To this end, we conducted an experimental and computational study focused on elucidating the precise mechanisms responsible for *cis*-selectivity and tacticity in Ru-based catalysts such as **1** and **2** by determining how variation of the cyclometalated group, *N*-aryl substituent, and X-type ligand affects the resulting polymer microstructure. Herein, we report the results of these mechanistic studies and propose a general model for *cis*-selectivity and tacticity for cyclometalated Ru-based initiators. These results provide a fundamental understanding of the mode-of-action of these catalysts and, as such, are generally

applicable to other transformations mediated by cyclometalated Ru-based catalysts.

RESULTS AND DISCUSSION

General Reactivity, *cis*-Selectivity, and Blockiness of ROMP Polymers Produced by Initiators 1–8. Reactions of a variety of cyclometalated catalysts (**1–8**, Figure 3) with

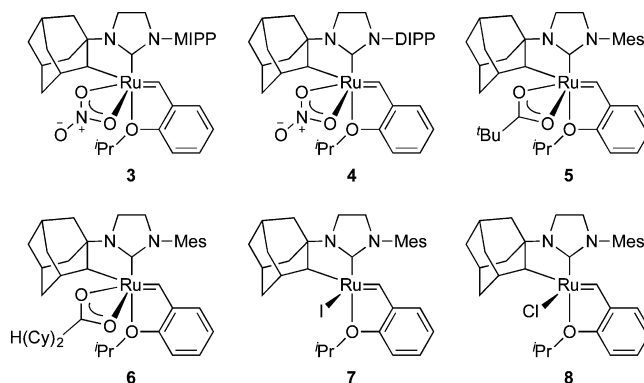
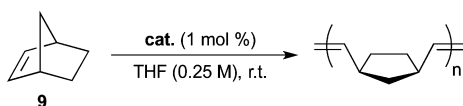


Figure 3. Catalysts **3–8**: MIPP = 2,6-methylisopropylphenyl (**3**); DIPP = 2,6-diisopropylphenyl (**4**); Mes = 2,4,6-trimethylphenyl (**5–8**).

norbornene (NBE, **9**) were screened to study general reactivity and *cis*-selectivity.¹¹ All polymerizations were performed at room temperature (rt) in THF (0.25 M) at a ratio of [monomer]/[initiator] = 100 (1 mol %). In general, catalysts **1–8** were found to yield polymers with moderate to high *cis* contents ($\sigma_c > 0.95$ in many cases) (Table 1).¹²

In the case of poly(NBE) and related polymers, the distribution of *cis* and *trans* double bonds in a given chain can be readily determined from ¹³C NMR, which provides information on the proportions of double-bond dyads in the polymer.^{11b,13} This distribution, known as blockiness, is represented by the relationship $r_t r_c$, where $r_t = (tt)/(tc)$ and $r_c = (cc)/(ct)$. Understanding the nature of the double bond distribution in any ROMP polymer affords significant mechanistic insight: a random distribution, characterized by $r_t r_c = 1$, suggests that the formation of a *cis* double bond is independent of any previously formed double bonds, whereas a blocky distribution ($r_t r_c > 1$) may indicate some influence of the polymer chain in the propagation step (i.e., chain-end control).

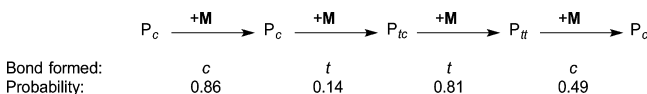
In general, predominantly *cis* (>50%) polymers of norbornene and related monomers formed by early generation

Table 1. Polymerization of Norbornene (9) with Catalysts 1–8

catalyst	σ_c^a	r_t^b	r_c^b	$r_t r_c$
1	0.97	—	—	—
2	0.92	0.27	6.5	1.7
3	0.97	—	—	—
4	0.99	—	—	—
5	0.74	0.52	2.4	1.2
6	0.74	0.94	3.9	3.7
7	0.88	0.45	6.5	2.9
8	0.82	0.53	4.8	2.5

^aFraction of double bonds having *cis* configuration; average of four values derived from $C_{2,3}$, $C_{1,4}$, $C_{7\gamma}$, and $C_{5,6}$ resonances, with agreement generally within ± 0.02 . ^bAverage of two values derived from $C_{1,4}$ and $C_{5,6}$ peaks.

ROMP catalysts are somewhat-to-highly blocky, with values of $r_t r_c$ ranging from 5 to 8 or more.^{13a} Significantly, r_t is almost always greater than 1 (i.e., $tt > tc$), indicating a preference for *trans* double bonds to occur in pairs. One postulate for this observed behavior is the existence of multiple kinetically distinct propagating species each having a different selectivity for the formation of *cis* or *trans* double bonds. This is supported by careful examination of the proportions of double bond triads in the polymers (readily derived from the known proportions of dyads), from which it can be shown that in the classical systems, the probability of *cis* or *trans* double bond formation at any given propagation step varies greatly depending on the identity of the last- and/or second-to-last formed double bond, presumably due to some interaction of these recently formed double bonds with the metal center or alkylidene.¹⁴ Propagating species in which the most recently formed double bond is *cis* (P_c) are highly *cis*-directing, whereas the selectivity of species in which the last-formed double bond is *trans* depends on whether the configuration of the penultimate double bond is *cis* (P_{tc} , highly *trans*-directing) or *trans* (P_{tt} , essentially nonselective) (Scheme 1).^{2b} These relative

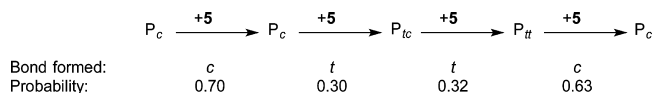
Scheme 1. Probabilities of Forming *cis* or *trans* Double Bonds in the $W(CO)_6/h\nu$ -Catalyzed ROMP of Norbornene (9)^a

^a P_c refers to a propagating species that has just formed a *cis* double bond, while P_{tc} and P_{tt} describe species that have just formed a *trans* double bond but have different penultimate double bonds (*cis* and *trans*, respectively). Adapted with permission from ref 2b. Copyright 1997 Academic Press.

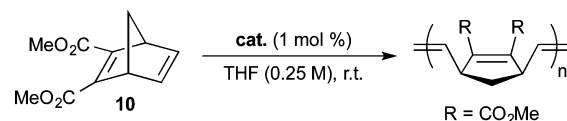
selectivities are ultimately responsible for the high incidence of *trans*–*trans* double bond pairs observed in poly(NBE) samples produced by classical metathesis catalysts.

Values of $r_t r_c$ calculated for the poly(NBE)s produced by catalysts 1–8 ranged from 1.25 to 3.70 (Table 1), indicating only modest deviations from randomness in the *cis*/*trans* double bond distributions of the polymers. Moreover, all of the highly *cis* polymers produced by catalysts 1–8 had r_t values that

were less than unity; in conjunction with the overall low values of $r_t r_c$, these low r_t values suggest that *trans* double bonds occur as single, random errors throughout the polymers rather than in pairs as observed with the classical systems. Furthermore, calculation of the probabilities of forming a *cis* or *trans* double bond according to the identity of the last- or last-but-one double bond revealed no significant dependence of *cis*-selectivity on the configurations of these previously formed double bonds in the polymerization of norbornene (Scheme 2). This suggests that chain-end control is most likely not the driving force behind the stereoselectivity in ROMP observed with initiators 1–8.

Scheme 2. Probabilities of Forming *cis* or *trans* Double Bonds in the ROMP of Norbornene (9) by Catalyst 5 ($\sigma_c = 0.74$)

Tacticity and Head–Tail Bias of ROMP Polymers Yielded by Catalysts 1–8. To fully understand the origins of selectivity in cyclometalated catalysts 1–8, a complete microstructural picture, taking into account not only *cis*/*trans* content but also tacticity and, in some cases, head–tail selectivity across dyads and triads, is essential. We therefore first turned our attention toward more complex monomers that could be used to quantify the extent of tacticity in polymers produced by these initiators. 2,3-Dicarbomethoxynorbornadiene (DCMNBD, 10) has been used extensively for this purpose, as the *cis* $C_{1,4}$ peak displays *m/r* splitting that is sufficiently resolved for quantitative analysis.¹⁵ Accordingly, for polymerizations of 10 with catalysts 1–8, the fraction of *cis*, r dyads in each highly *cis* polymer was easily determined, as shown in Table 2. Surprisingly, the *cis* portions of the polymers

Table 2. Polymerization of Monomer 10 with Catalysts 1–8

catalyst	σ_c^a	% r (<i>cis</i>) ^b
1	0.99	99
2	0.87	85
3	0.84	84
4	0.91	85
5	0.72	68
6	0.65	68
7	0.98	96
8	0.94	96

^aFraction of double bonds having *cis* configuration; average of two values derived from $C_{2,3}$ and $C_{1,4}$ resonances, with agreement generally within ± 0.02 . ^bDerived from *cis* $C_{1,4}$ peaks.

produced by catalysts 2–8 were found to be highly syndiotactic and not atactic as previously thought (Figure 4). In fact, monodentate catalysts 7 and 8 yielded polymers with almost exclusively a single structure (*cis*, *syndiotactic*).

We next probed the effects of temperature and dilution on the polymerization of 10 by initiator 2. If the propagation reaction is in competition with other processes occurring at the

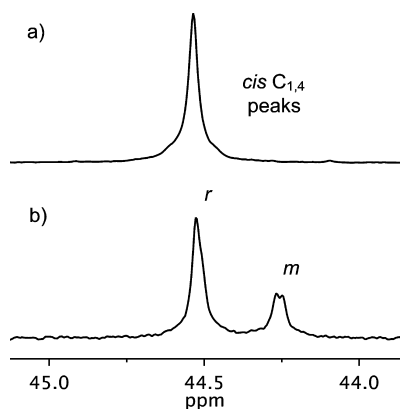


Figure 4. ^{13}C NMR spectra of (a) *cis,syndiotactic* poly(**10**) produced by catalyst **1** and (b) 72% *cis*, 68% *syndiotactic* (*cis* regions) poly(**10**) produced by catalyst **5**.

catalyst center, such as alkylidene isomerization, changes in *cis* content and/or tacticity can result from variations in temperature or monomer concentration.^{3b} Decreasing monomer concentration in particular presents a simple method in which to slow propagation relative to these other processes. However, we found that the concentration of **10** had very little appreciable effect on the microstructures of the polymers produced by catalyst **2** (Table 3). Increasing the temperature

Table 3. Temperature and Concentration Effects on the Polymerization of Monomer 10 with Catalyst 2

temp (°C)	conc (M)	σ_c^a	% <i>r</i> (<i>cis</i>) ^b
25	0.25	0.87	85
0	0.25	0.92	90
40	0.25	0.83	81
25	0.05	0.90	88
25	1.25	0.88	85

^aFraction of double bonds having *cis* configuration; average of two values derived from $\text{C}_{2,3}$ and $\text{C}_{1,4}$ resonances, with agreement generally within ± 0.02 . ^bDerived from *cis* $\text{C}_{1,4}$ peaks.

from 25 to 40 °C, on the other hand, resulted in an approximately 5% decrease in both the *cis* content and the tacticity of poly(**10**)/**2**, while decreasing the temperature to 0 °C had the opposite effect. These results suggest that alkylidene isomerization might indeed be occurring at a rate comparable to (or faster than) that of propagation and could therefore feasibly be a major contributor in the resulting stereoselectivity of the polymerization.

As catalysts **1**, **2**, and **4** were found to cover the general range of microstructures produced by **1**–**8**, further polymerizations were performed using only these three systems. Results similar to monomer **10** were obtained when 2,3-bis(trifluoromethyl)-norbornadiene (**11**) was polymerized using catalysts **1**, **2**, and **4** (Table 4);¹⁶ the resulting polymers were also *cis*-biased with highly syndiotactic *cis* regions.

To obtain a comprehensive understanding of the origins of *cis*-selectivity and tacticity in cyclometalated catalysts **1**–**8**, it is necessary to also determine the tacticity of the *trans* regions of polymers derived from these systems. However, the *trans* peaks in polymers derived from monomers **10** and **11** are too small and not sufficiently resolved for meaningful analysis. Thus, we next turned our attention toward polymers with more easily analyzable *trans* regions, *exo,exo*-7-oxa-5-norbornene-2,3-dicar-

Table 4. Polymerization of Monomer 11 with Catalysts 1, 2, and 4

catalyst	σ_c^a	% <i>r</i> (<i>cis</i>) ^b
1	0.79	99
2	0.63	99
4	0.55	>99

^aFraction of double bonds having *cis* configuration; average of three values derived from $\text{C}_{2,3}$, $\text{C}_{1,4}$, and C_7 resonances, with agreement generally within ± 0.02 . ^bDerived from *cis* C_7 peaks.

Table 5. Polymerization of Monomer 12 with Catalysts 1, 2, and 4

catalyst	σ_c^a
1	0.94
2	0.73
4	0.93

^aFraction of double bonds having *cis* configuration; average of three values derived from CO_2Me , $\text{C}_{2,3}$, and $\text{C}_{1,4}$ resonances, with agreement generally within ± 0.03 .

^aFraction of double bonds having *cis* configuration; average of three values derived from CO_2Me , $\text{C}_{2,3}$, and $\text{C}_{1,4}$ resonances, with agreement generally within ± 0.03 .

boxylic acid (**12**) and 7-methylnorbornene (7-MNBE, **13**).^{15,17} Polymers produced from **12** had generally lower *cis* contents ($\sigma_c = 0.73$ – 0.94) (Table 5), allowing for facile qualitative analysis of the *trans* portions via the *trans* $\text{C}_{1,4}$ peak, which displays *m/r* tacticity splitting. Although the *cis* peaks are not sensitive to tacticity splitting, a tacticity bias can be determined on the basis of comparison with data from catalyst **1**, shown to consistently produce predominantly syndiotactic polymers.⁹ All of the polymers produced by catalysts **1**, **2**, and **4** contained syndiotactic-biased *cis* regions. The tacticities of *trans* regions, however, were found to differ somewhat depending on the specific catalyst/monomer combination being studied. Catalysts **1** and **4** produced polymers with *trans* regions that were largely syndiotactic, while polymer produced by catalyst **2** appeared to have negligible bias for either *m* or *r* dyads in the *trans* regions (Figure 5).

Next, we exposed catalysts **1**, **2**, and **4** to a 1.2:1 *syn/anti* mixture of **13**. It is generally accepted that norbornene and related compounds react at the less-hindered *exo* face in ROMP.¹⁸ This was confirmed for catalysts **1** and **2** by the polymerization of **13**; both polymerized the *anti* monomer almost exclusively (<2% *syn*-derived polymer was observed by ^{13}C NMR). This occurs because the 7-methyl group in the *syn* monomer is positioned directly over the *exo* face of the double bond, and as such, polymerization via *exo* attack is prohibitively high in energy, whereas this is avoided in the *anti* monomer. Gratifyingly, unambiguous determination of tacticity was achieved for both the *cis* and the *trans* regions by analyzing polymers of *anti*-**13**, in which all of the carbons with the exception of C_7 are sensitive to tacticity. Samples of poly(*anti*-7-MNBE) produced by catalysts **1** and **2** were discovered to have highly syndiotactic *cis* regions (90–95% *r*) and highly syndiotactic *trans* regions (96–99% *r*) (Table 6). No

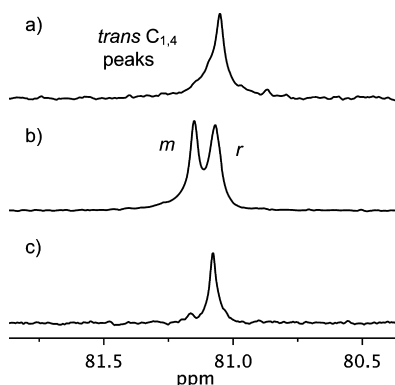
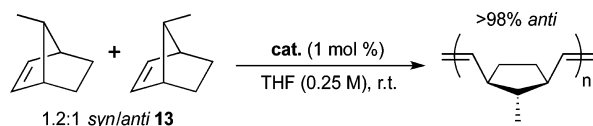


Figure 5. ^{13}C NMR spectra highlighting the *trans* $\text{C}_{1,4}$ regions of (a) 94% *cis* poly(**12**) produced by catalyst **1**, (b) 73% *cis* poly(**12**) produced by catalyst **2**, and (c) 93% *cis* poly(**12**) produced by catalyst **4**.

Table 6. Polymerization of a 1.2:1 *syn/anti* Mixture of 7-Methylnorbornene (**13**) with Catalysts **1**, **2**, and **4**



catalyst	σ_c^a	tacticity ^b
1	0.97	<i>cis</i> regions, 95% <i>r</i> ; <i>trans</i> , >99% <i>r</i>
2	0.87	<i>cis</i> , 90% <i>r</i> ; <i>trans</i> , >99% <i>r</i>
4 ^c	—	—

^aFraction of double bonds having *cis* configuration; derived from $\text{C}_{1,4}$ resonances. ^bDerived from *cis* and *trans* $\text{C}_{1,4}$ peaks. ^cNo reaction.

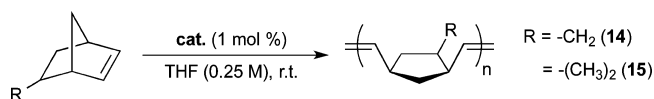
appreciable amount of polymer was formed with initiator **4**; this is likely a result of the increased steric bulk associated with the *N*-2,6-diisopropylphenyl group of this catalyst.

Finally, we probed the extent of head-to-tail (HT) selectivity exhibited by catalysts **1**, **2**, and **4** in the polymerization of unsymmetrically substituted norbornenes. HT bias is measured by determining the ratios of head–head/head–tail (HH/HT) and tail–tail/tail–head (TT/TH) dyads in both the *cis* and the *trans* regions. The enantiomers are randomly distributed throughout the polymer when these values are equal to unity (i.e., no bias is present).

The degree of HT bias in polymers derived from substituted norbornenes is delicately related to electronic and steric effects associated with both the monomer substituent(s) and the catalyst. Additionally, any catalyst relaxation or isomerization processes occurring on the same time scale as propagation may also contribute to HT bias, as different propagating species can exhibit different levels of H/T discrimination. One way to probe the role of the catalyst in HT selectivity is via the polymerization of norbornene monomers substituted at the C_5 or C_6 position. These substituents are sufficiently remote from the double bond that they generally do not exert any intrinsic head-to-tail bias resulting from steric effects; thus, any observed bias with these monomers is likely catalyst-dependent. An HT bias in the polymerization of C_5 - and C_6 -substituted norbornene monomers with a given catalyst, then, particularly one that increases with decreasing rate of polymerization (or increasing dilution), may point toward the existence of two or more distinct propagating species with distinctive HT biases.^{3b}

To test for HT-bias, catalysts **1**, **2**, and **4** were used to polymerize from the unsymmetrically substituted racemic monomers 5-methylene-2-norbornene (**14**) and 5,5-dimethylnorbornene (DMNBE, **15**).^{19,20} Although all of the catalysts were found to be essentially bias-free in the polymerization of monomer **14** (*cis* TT/TH ratios = 0.93–1.04), initiators **1** and **2** displayed more significant biases in the polymerization of **15** (*cis* TT/TH ratios = 1.11–1.51; *trans* TT/TH ratios = 0.20–1.00) (Table 7). Notably, the rate of polymerization of

Table 7. Polymerization of Monomers **14** and **15** with Catalysts **1**, **2**, and **4**



catalyst	monomer	σ_c^a	<i>cis</i> TT/TH ^b	<i>trans</i> TT/TH ^c
1	14	0.98	0.93	— ^d
2	14	0.87	0.95	—
4	14	0.94	1.0	—
1	15	0.78	1.1	0.20
2	15	0.77	1.5	0.50
4 ^e	—	—	—	—

^aFraction of double bonds having *cis* configuration; derived from C_6 resonances (**14**) and C_2 resonances (**15**). ^bDerived from *cis* TT and TH $\text{C}_{2,3}$ peaks (**14**) and *cis* TT and TH C_2 peaks (**15**). ^cDerived from *trans* TT and TH C_2 peaks (**15**). ^dHere and below: overlap of *trans* TT and HH $\text{C}_{2,3}$ peaks in poly(**14**) precluded *trans* TT/TH or HH/TT analysis. ^eNo reaction.

monomer **15** by initiators **1** and **2** was significantly lower than that of **14** (1–4 h to full conversion vs minutes), and as seen with monomer **13** no appreciable amount of poly(**15**) was formed using catalyst **4** (likely as a consequence of the increased steric hindrance imparted by the *endo* substitution in monomer **15**). The increase in HT bias with decreasing rate suggests that there is more than one propagating species (resulting from alkylidene isomerization or a similar process), each with a different inherent HT bias.

Computational Investigations of Reaction Pathways and Proposed Model for *cis*-Selectivity and Tacticity in Catalysts **1–**8**.** The selectivity for *cis,syndiotactic* polymers exhibited by catalysts **1**–**8** is hypothesized to be a result of stereogenic metal control, as in the case of the Mo- and W-based MAP alkylidene complexes described earlier. Because initiators **1**–**8** are stereogenic-at-Ru, the absolute configuration of the metal center is inverted with each propagation step to generate enantiomeric (in the case of **1**) or diastereomeric (**2**–**8**) carbenes (Figure 6), resulting in the addition of incoming monomers to alternating sides of the Ru=C bond.

Previous computational and experimental work has shown that *cis*-selectivity in cross metathesis reactions using cyclo-metallated catalysts similar to **1** and **2** stems from the steric influence of the bulky *N*-aryl group positioned directly over the side-bound metallacycle, which results in the destabilization of the transition state leading to the formation of *trans* olefins.²¹ It is likely that monomer approach in ROMP is similarly influenced by the presence of the *N*-aryl group, in that norbornene and related derivatives would be expected to react at the less hindered *exo* face with the methylene bridge pointed away from the *N*-aryl “cap”.²² In the terminology employed by Schrock and co-workers in regards to well-defined Mo and W initiators, this approach is designated *anti*, in that the bulk of

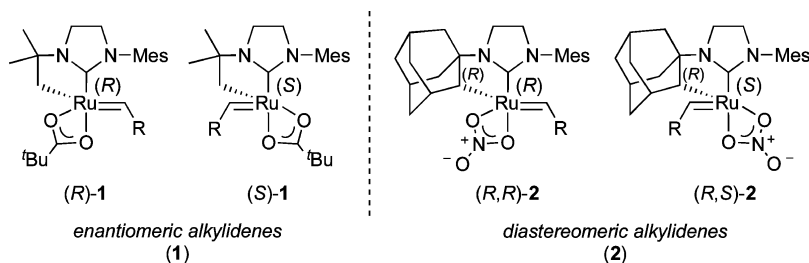
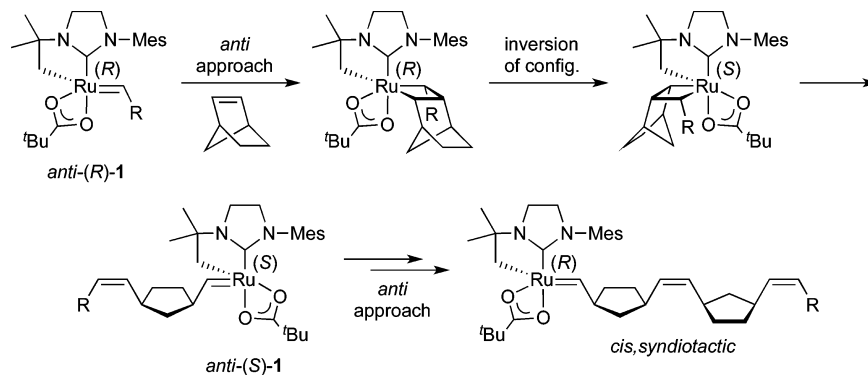


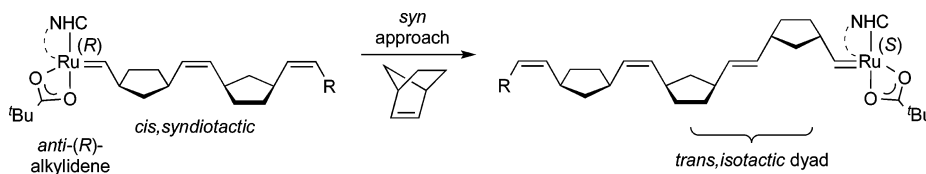
Figure 6. Enantiomeric (1) and diastereomeric (2) alkyldenes generated by the stereochemical inversion of the Ru metal center that occurs with each forward metathesis step.

Scheme 3. Proposed Mechanism for Forming *cis,syndiotactic* Polymers Using Cyclometalated Catalyst 1^a



^aMes = 2,4,6-trimethylphenyl, R = *o*-isopropoxyphenyl.

Scheme 4. Formation of a *trans,isotactic* Dyad in a Predominantly *cis,syndiotactic* Polymer Following a *syn* Approach of the Monomer to an *anti* Alkyldene^a



^aR = *o*-isopropoxyphenyl.

the monomer points away from the *N*-aryl group; the opposite approach is *syn*.^{5c} Likewise, *syn* and *anti* Ru=CHR isomers are defined according to whether the R group of the alkyldene points toward or away from the *N*-aryl group. A consistently *anti* monomer approach to alternate sides of an *anti* alkyldene as a result of stereogenic metal control leads to the formation of a *cis,syndiotactic* polymer (Scheme 3). However, if the incoming monomer were to occasionally adopt a *syn* approach to the *anti* alkyldene, a *trans,isotactic* dyad “error” would be produced (Scheme 4).

Mixed tacticities (i.e., *cis,isotactic* and *trans,syndiotactic* dyads) would result if isomerization of the *anti* alkyldene were to occur between propagation steps, either through rotation about the M=C double bond to adopt a *syn* configuration or via a nonmetathesis-based polytopal rearrangement²³ between the stereoisomeric metal alkyldenes (i.e., (R)-1 and (S)-1). Moreover, the degree to which these “errors” occur would be related to the barrier to these processes, with an increase in regions of mixed tacticity being evidenced when the rate of alkyldene isomerization occurs on a time scale that is comparable to the time scale for propagation. Competition between alkyldene isomerization and propagation would also provide a reasonable explanation for the HT bias detected in

catalysts 1 and 2, as well as the temperature effect observed in the polymerization of 10 with catalyst 2, as outlined previously.

To explore these possible alkyldene isomerization processes, as well as to better understand how they may lead to a loss in *cis*-selectivity and tacticity in some of these cyclometalated ruthenium-based systems, DFT calculations on polymerization reactions involving catalysts 1 and 2 were performed.²⁴ All calculations were performed with Gaussian 09²⁵ at the M06/SDD-6-311+G(d,p)/SMD(THF)//B3LYP/SDD-6-31G(d) level of theory. See the Supporting Information for computational details.

We first investigated the likelihood of alkyldene isomerization through a nonmetathesis-based polytopal rearrangement pathway. The computed energy profile of the polytopal rearrangement of *N*-*t*Bu-cyclometalated ruthenium alkyldene 16 to form its diastereomer 17 (using a 3-cyclopentenyl group as a model of the polymer chain) is shown in Figure 7. This multistep rearrangement process starts from alkyldene *anti* → *syn* isomerization via rotation (18-TS), which requires a relatively low barrier to form the *syn* alkyldene intermediate 19. Isomerization of the alkyldene to the position *trans* to the NHC leads to highly unstable intermediate 21. Complex 21 subsequently undergoes ring flip of the five-membered chelate

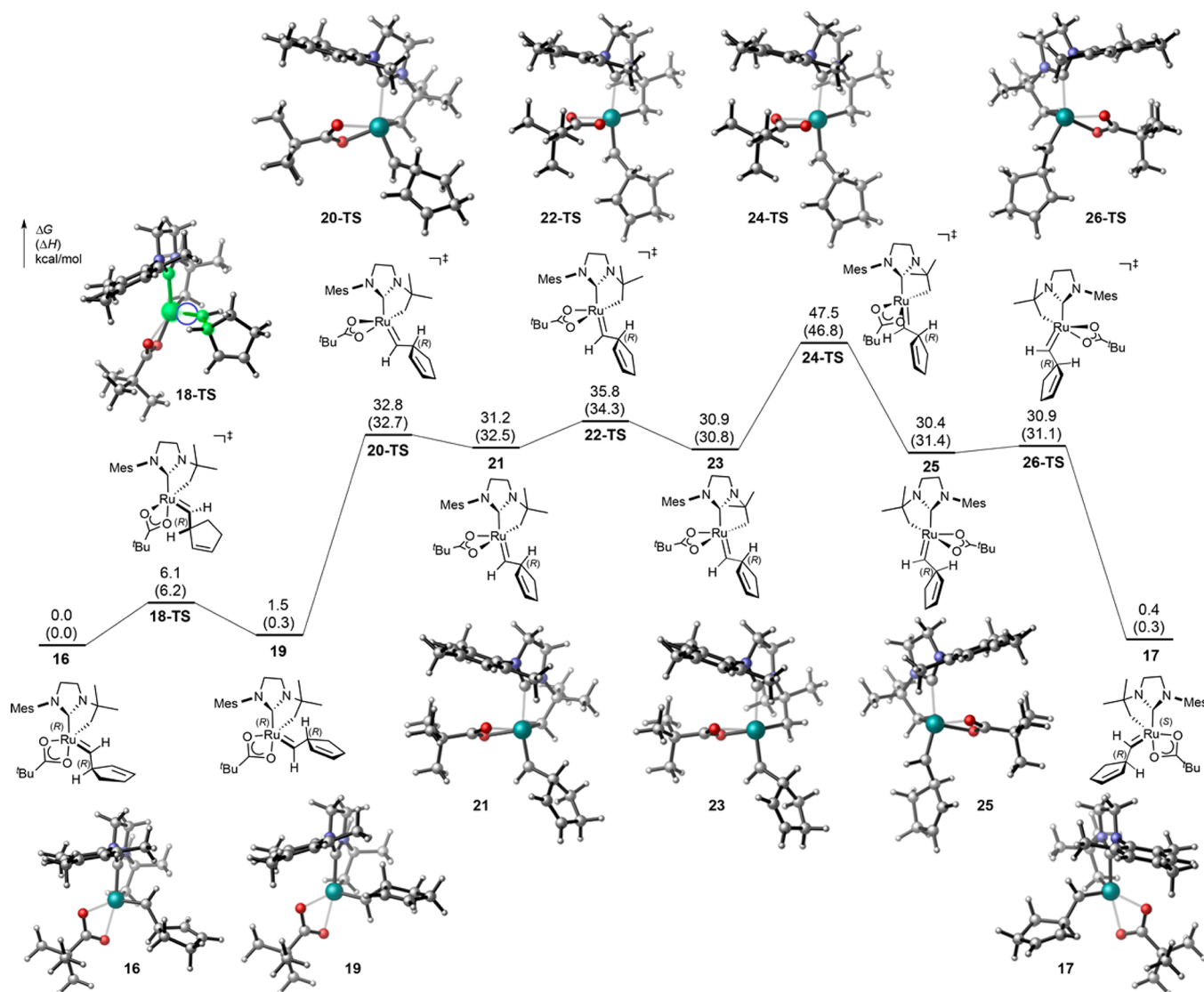


Figure 7. Nonmetathesis-based polytopal rearrangement of ruthenium alkylidene **16** to its diastereomer **17**.

(22-TS) and a very unfavorable rearrangement of the pivalate ligand (24-TS) to form complex **25**, which then isomerizes to **17**. With the alkylidene *trans* to the NHC ligand, complexes **21**, **23**, and **25** are all highly unstable, and this process is highly disfavored.

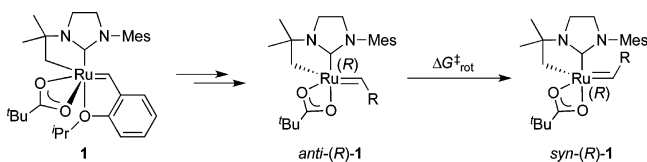
We next explored the probability of isomerization via rotation about the alkylidene Ru=C double bond. The computed rotational barriers for catalysts **1** and **2** are summarized in Table 8. Because of steric repulsions between the alkylidene R group and the *N*-aryl group, the *syn* alkylidene is less stable than the *anti* isomer. The alkylidene rotation barrier is only slightly affected by the steric bulk of the substituent on the alkylidene and the cyclometalated group on the catalyst. In general, the barrier to alkylidene rotation is comparable to the barrier for monomer addition (see below).

Given the high barrier and the unstable intermediates in the polytopal rearrangement process, we conclude that a nonmetathesis isomerization of the ruthenium alkylidene is highly unlikely to occur under the reaction conditions, and a pathway involving bond rotation about the Ru=C alkylidene is much more likely to be responsible for alkylidene isomerization. With this in mind, we can now complete our model for *cis*-selectivity

and tacticity in catalysts **1–8** by factoring in the effects of alkylidene rotation on the final polymer microstructure. In a predominantly *cis,syndiotactic* polymer resulting from stereogenic metal control, rotation of the alkylidene from *anti* to *syn* followed by monomer approach in either a *syn* or an *anti* fashion results in the formation of a *cis,isotactic* or *trans,syndiotactic* dyad, respectively (Scheme 5).

We next set out to explore the possible pathways leading to the formation of each type of dyad in more depth. We focused on the [2+2] cycloaddition step, as in reactions with norbornene and norbornadiene derivatives, the [2+2] cycloaddition step requires a significantly higher barrier than the [2+2] cycloelimination, and thus the [2+2] cycloaddition is effectively irreversible.^{24b,26} Importantly, *cis/trans*-selectivity and tacticity are both determined in the [2+2] cycloaddition step. The four possible transition states derived for the [2+2] cycloaddition of monomer **10** at the *exo* face to ruthenium alkylidene **27**, a model of the propagating species of the *N*-^tBu-cyclometalated catalyst **1**, are shown in Figure 8. Because isomerization between the *anti* and *syn* alkylidenes via rotation of the Ru=C bond occurs with a barrier comparable to that of propagation, monomer addition to both *anti* and *syn*

Table 8. Computed Alkylidene Rotational Barriers



catalyst	alkylidene	$\Delta G_{\text{rot}}^{\ddagger}$ ^a	$\Delta G_{(\text{syn-anti})}$ ^b
1		6.1	1.5
1	 E = CO ₂ Me	9.0	5.0
(R,R)-2	 E = CO ₂ Me	9.9	3.9
(R,S)-2	 E = CO ₂ Me	6.3	4.0

^aAlkylidene rotational barrier with respect to the *anti* alkylidene.

^bEnergy difference between *syn* and *anti* alkylidene isomers. All energies are in kcal/mol.

alkylidenes was computed (28-TS-A/B and 28-TS-C/D, respectively). In these transition states, the olefin approaches the catalyst from the side, that is, *cis* to the NHC ligand, in line with our previous computational study of olefin cross-metathesis with cyclometalated *cis*-selective ruthenium catalysts.²¹ The bottom-bound pathway, that is, olefin approaching *trans* to the NHC, and the addition to the *endo* face of the norbornadiene both require much higher activation energies (15–21 kcal/mol, see the Supporting Information for details).

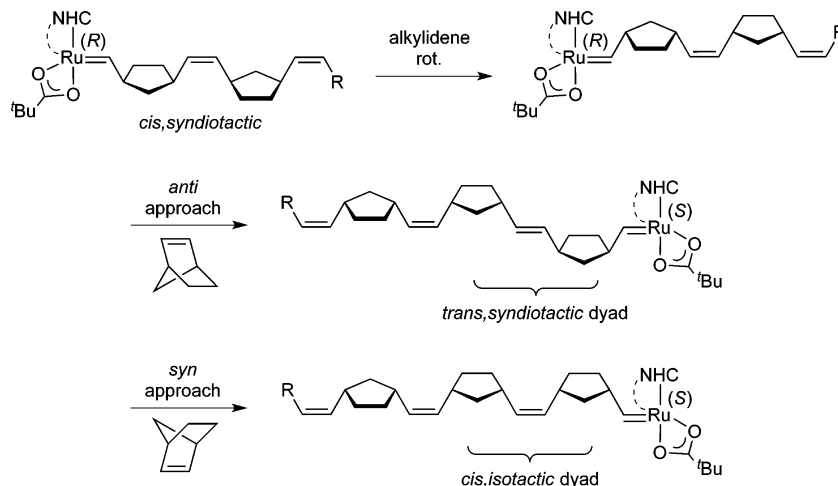
The most favorable [2+2] cycloaddition transition state is the one leading to the formation of a *cis,syndiotactic* dyad, 28-TS-A, in which the *anti* alkylidene reacts with a monomer approaching in an *anti* fashion. The ligand–substrate steric repulsions in this *anti/anti* approach are minimized due to the bulk of the monomer and the alkylidene both being directed away from the *N*-aryl group. The next lowest energy transition

state leads to the formation of a *trans,syndiotactic* arrangement (28-TS-C), in which the *syn* alkylidene reacts with a monomer approaching in an *anti* fashion. This *anti/syn* approach (28-TS-C) is 2.1 kcal/mol higher in energy than the *anti/anti* approach (28-TS-A), which is consistent with the high *cis*-selectivity observed experimentally. Both *trans,isotactic* and *cis,isotactic* dyads result when the monomer approaches in a *syn* fashion (28-TS-B and 28-TS-D, respectively), which requires much higher activation energies due to the repulsion of the methylene bridge with the *N*-aryl group. This is in agreement with the high syndiotacticity of both the *cis* and the *trans* regions observed experimentally in the polymerizations of monomers 12 and 13 (Tables 4 and 5).

Experimentally, the polymerization of monomer 10 with *N*-adamantyl cyclometalated ruthenium catalysts (2–8) is both less *cis*-selective and less syndioselective than that with the *N*-*t*-Bu cyclometalated catalyst 1 (Table 2). Interestingly, when the total content of *cis* double bonds in poly(10) is plotted against the percentage of *cis* double bonds in *cis,r* dyads for catalysts 1–8, a linear dependence is observed (Figure 9). Because the barriers to alkylidene rotation in catalysts 1 and 2 with monomer 10 are comparable (cf., Table 8), this relationship is likely a result of the relative differences in the energetics of the propagation transition states for each catalyst (which also determine both *cis*- and *syndio*-selectivity). Thus, the [2+2] cycloaddition transition states with monomer 10 and alkylidene 29, a model of the propagating species of catalyst 2, were calculated to further investigate the connection between *cis*-selectivity and tacticity in these systems.

With the asymmetric *N*-adamantyl-cyclometalated group on catalyst 2, an additional set of alkylidene diastereoisomers are possible, resulting in eight possible propagation transition states (Figure 10). In the more stable alkylidene diastereomer (R,R)-29, the Ru=C bond is *anti* to the alpha C–H bond on the cyclometalated carbon atom. In (R,S)-29, the Ru=C bond is *syn* to the alpha C–H bond. As discussed above, direct isomerization between (R,R)-29 and (R,S)-29 via polytopal rearrangement is not possible. Instead, the configuration of ruthenium alternates between (R,R)-29 and (R,S)-29 after each monomer addition.

Scheme 5. Formation of a *trans,syndiotactic* or *cis,isotactic* Dyad Resulting from an *anti* or *syn* Monomer Approach, Respectively, to a *syn* Alkylidene Following Alkylidene Rotation (*anti* to *syn*) in a Predominantly *cis,syndiotactic* Polymer^a



^aR = *o*-isopropoxyphenyl.

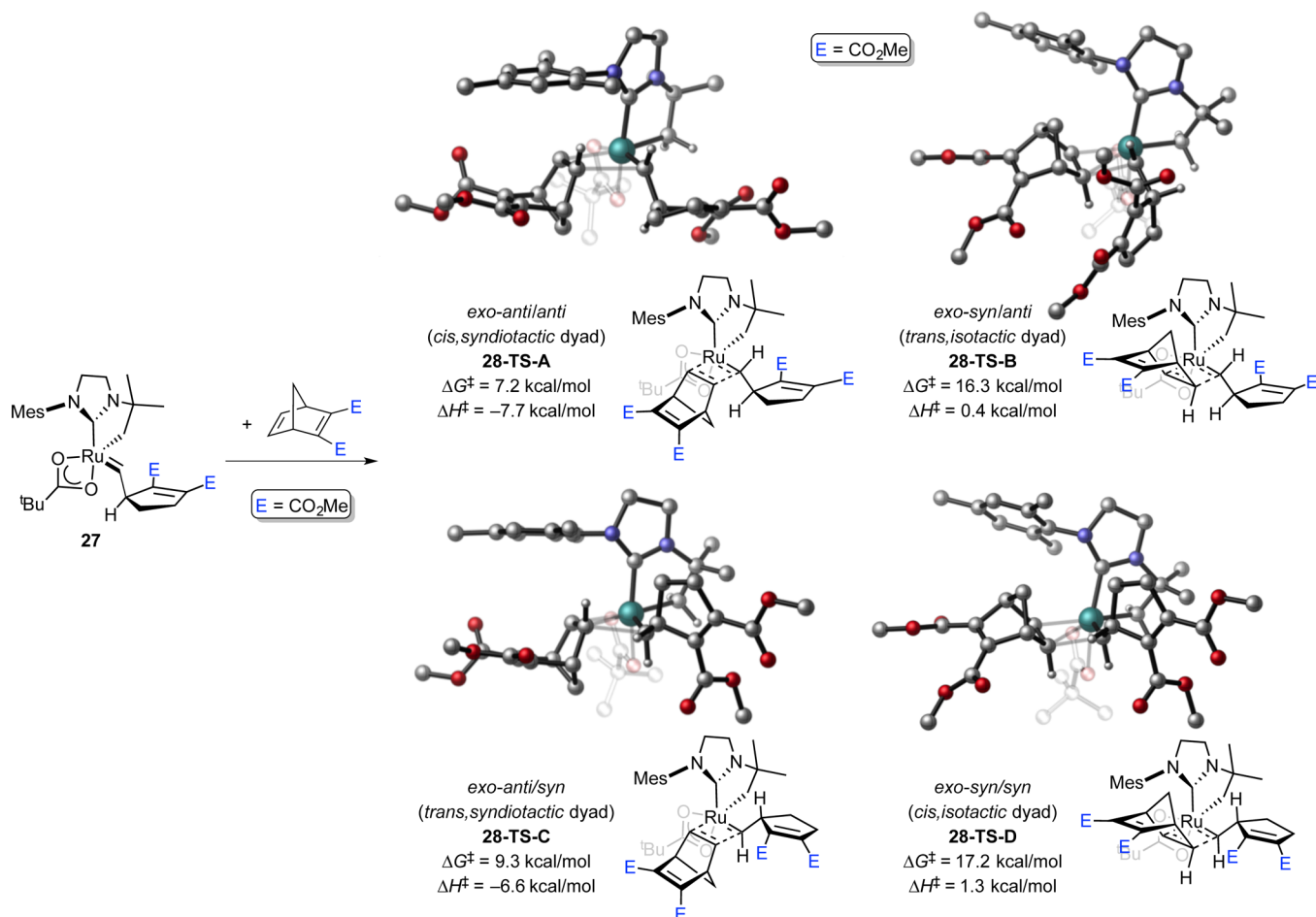


Figure 8. [2+2] cycloaddition transition states for the polymerization of monomer 10 with catalyst 27. Energies are with respect to the separated ruthenium alkyldiene and monomer 10.

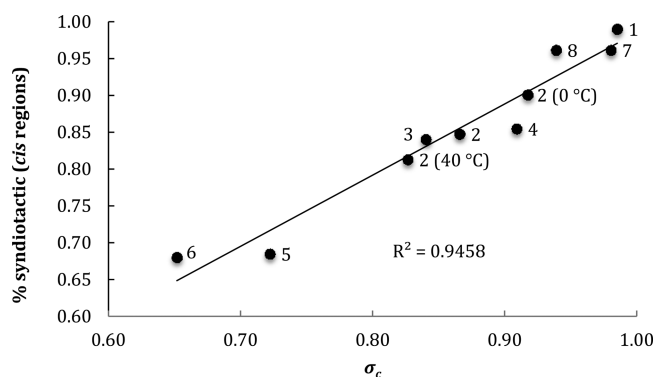


Figure 9. Linear relationship between *cis* content and tacticity of the *cis* regions in poly(DCMNBD) [poly(10)] for catalysts 1–8 (data obtained from Table 2).

Similar to the reaction with catalyst 1, the *cis,syndio*-selective *anti/anti* approach is the most favorable with catalyst 2 (30-TS-A and 31-TS-A for the addition to alkyldiene (*R,R*)-29 and (*R,S*)-29, respectively). However, the corresponding *trans,syndio*-selective transition states 30-TS-C and 31-TS-C are only 0.7 and 2.0 kcal/mol less stable, respectively. Similarly, the transition states leading to the formation of *trans,isotactic* and *cis,isotactic* dyads (30-TS-B/D and 31-TS-B/D, respectively), while still highly unfavorable, are also less destabilized relative to *cis,syndio*-selective 30-TS-A and 31-TS-A. The lower

selectivity for *cis,syndiotactic* dyads is attributed to the increased steric repulsion between the alkyldiene R group and the bulkier cyclometalated *N*-adamantyl group in the *cis,syndio*-selective transition states, in particular in 30-TS-A where the steric bulk of the adamantyl chelate is closer to the R group than in 31-TS-A. This conclusion likely extends to the other cyclometalated-*N*-adamantyl initiators 3–8.

CONCLUSION

A series of cyclometalated Ru-based metathesis initiators were evaluated in the ring-opening metathesis polymerization (ROMP) of a variety of norbornene- and norbornadiene-derived monomers. Highly *cis,syndiotactic* polymers were generated in most cases. In polymers with an imperfect microstructure, the major errors were in the form of *cis,isotactic* and *trans,syndiotactic* regions. Using experimental and computational insights, a model was developed to explain the pattern of stereoselectivity exhibited by this family of catalysts in ROMP. The near-perfect *cis,syndio*-selectivity of these systems is postulated to arise from the inversion of configuration at the metal center that occurs with each propagation step (i.e., stereogenic metal control), in conjunction with an almost exclusive approach of the monomer in an *anti* fashion to the energetically preferred *anti* alkyldiene. The majority of microstructural errors are likely a result of interconversion between *syn* and *anti* alkyldiene isomers in the propagating catalytic species. Addition of the monomer in an *anti* or *syn*

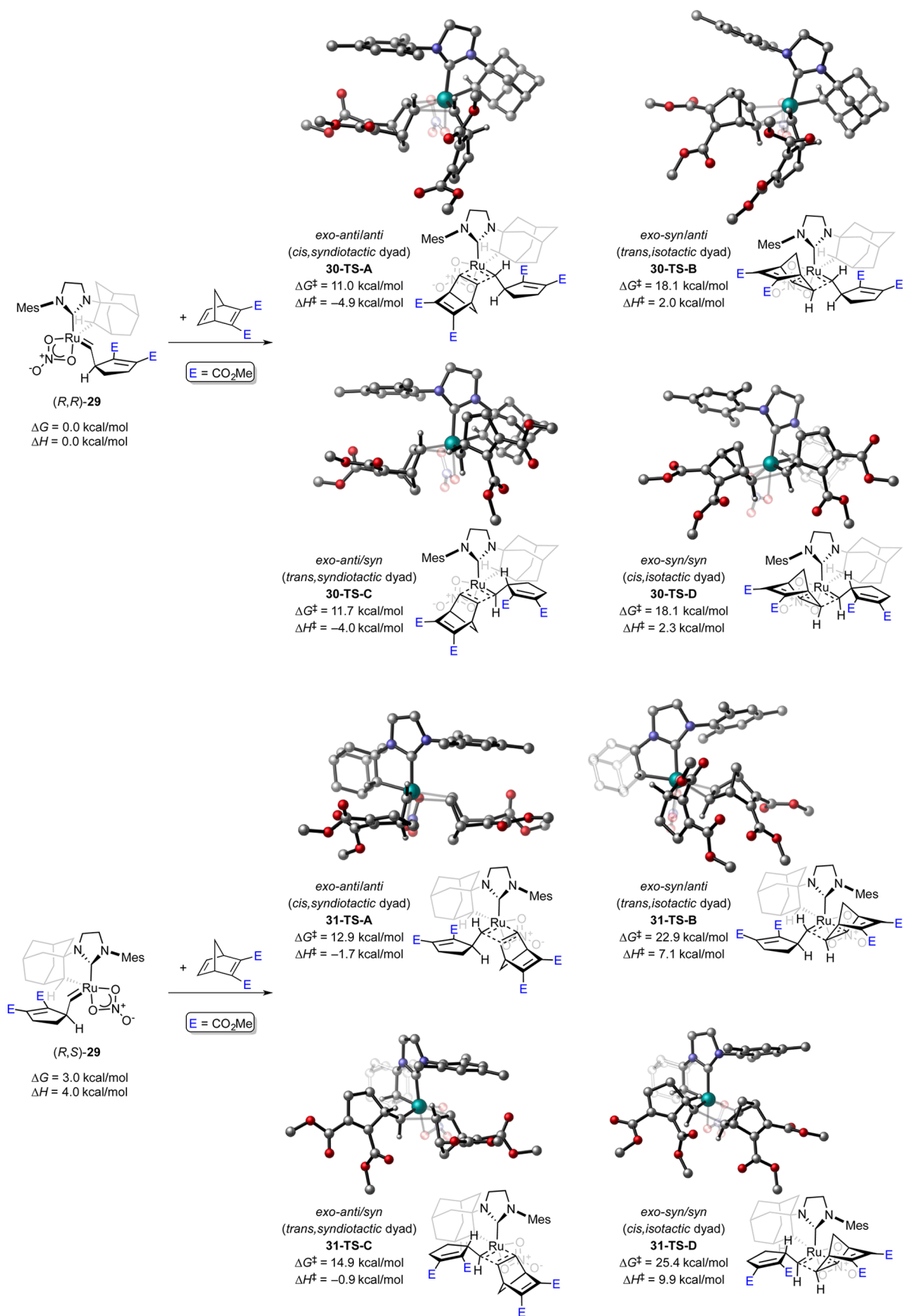


Figure 10. [2+2] cycloaddition transition states for the polymerization of monomer **10** with catalyst **29**. Energies are with respect to the separated ruthenium alkylidene and monomer **10**.

fashion to the higher energy *syn* alkylidene leads to the formation of a *trans,syndiotactic* or *cis,isotactic* dyad, respectively. Finally, the highest *cis,syndio*-selectivity was exhibited by a catalyst containing a cyclometalated *N*⁴Bu group. This was determined to originate from the decreased steric environment in this catalyst relative to the *N*-adamantyl-cyclometalated catalysts, as increased substitution close to the metal center is shown to minimize the differences in energy between transition states. The mechanistic insights gained in this study will not only aid in the development of new and improved *cis*-selective Ru-based catalysts, but also provide increased predictive power in synthetic transformations mediated by these systems.

■ ASSOCIATED CONTENT

Supporting Information

The Supporting Information is available free of charge on the ACS Publications website at DOI: 10.1021/jacs.5b12277.

Experimental details, NMR spectra, and details of computational methods and additional computational results (PDF)

■ AUTHOR INFORMATION

Corresponding Authors

*houk@chem.ucla.edu

*rhg@caltech.edu

Notes

The authors declare no competing financial interest.

■ ACKNOWLEDGMENTS

We thank Dr. David VanderVelde for his assistance with NMR experimentation and analysis. This work was financially supported by the NIH (R01GM031332), ONR (N000141310895), NSF (CHE-1361104, K.N.H.), NDSEG (fellowship to L.E.R.), NSF-GRFP (fellowship to T.S.A.), and NSERC (fellowship to V.M.M.). Materia, Inc. is thanked for its generous donation of metathesis catalysts. Calculations were performed on the Hoffman2 cluster at UCLA and the Extreme Science and Engineering Discovery Environment (XSEDE), which is supported by the NSF (OCI-1053575).

■ REFERENCES

- (1) (a) Haas, F.; Theisen, D. *Kautsch. Gummi Kunstst.* **1970**, *23*, 502. (b) Edwards, J. H.; Feast, W. J.; Bott, D. C. *Polymer* **1984**, *25*, 395. (c) Ofstead, E. A. *Encyclopedia of Polymer Science and Engineering*, 2nd ed.; Wiley: New York, 1988; Vol. 11. (d) Park, L. Y.; Schrock, R. R.; Stieglitz, S. G.; Crowe, W. E. *Macromolecules* **1991**, *24*, 3489. (e) Dounis, P.; Feast, W. J.; Kenwright, A. M. *Polymer* **1995**, *36*, 2787. (f) Lee, C.; Wong, K.; Lam, W.; Tang, B. *Chem. Phys. Lett.* **1999**, *307*, 67. (g) Wong, K. S.; Lee, C. W.; Zang, B. Z. *Synth. Met.* **1999**, *101*, 505.
- (2) (a) Hamilton, J. G. Stereoselectivity in Ring-Opening Metathesis Polymerization. In *Handbook of Metathesis*; Grubbs, R. H., Ed.; Wiley-VCH: Weinheim, Germany, 2003; Vol. 3, pp 143–179. (b) Ivin, K. J.; Mol, J. C. Ring-Opening Metathesis Polymerization: General Aspects. *Olefin Metathesis and Metathesis Polymerization*; Academic Press: San Diego, CA, 1997; pp 224–259.
- (3) (a) Schrock, R. R. *Dalton Trans.* **2011**, *40*, 7484. (b) Schrock, R. R. *Acc. Chem. Res.* **2014**, *47*, 2457.
- (4) (a) McConville, D. H.; Wolf, J. R.; Schrock, R. R. *J. Am. Chem. Soc.* **1993**, *115*, 4413. (b) O'Dell, R.; McConville, D. H.; Hofmeister, G. E.; Schrock, R. R. *J. Am. Chem. Soc.* **1994**, *116*, 3414. (c) Schrock, R. R.; Lee, J. K.; O'Dell, R.; Oskam, J. H. *Macromolecules* **1995**, *28*, 5933. (d) Totland, K. M.; Boyd, T. J.; Lavoie, G. G.; Davis, W. M.; Schrock, R. R. *Macromolecules* **1996**, *29*, 6114.

- (5) (a) Flook, M. M.; Jiang, A. J.; Schrock, R. R.; Müller, P.; Hoveyda, A. H. *J. Am. Chem. Soc.* **2009**, *131*, 7962. (b) Flook, M. M.; Ng, V. W. L.; Schrock, R. R. *J. Am. Chem. Soc.* **2011**, *133*, 1784. (c) Flook, M. M.; Börner, J.; Kilyanek, S. M.; Gerber, L. C. H.; Schrock, R. R. *Organometallics* **2012**, *31*, 6231. (d) Forrest, W. P.; Axtell, J. C.; Schrock, R. R. *Organometallics* **2014**, *33*, 2313. (e) Forrest, W. P.; Weis, J. G.; John, J. M.; Axtell, J. C.; Simpson, J. H.; Swager, T. M.; Schrock, R. R. *J. Am. Chem. Soc.* **2014**, *136*, 10910.
- (6) Bazan, G. C.; Khosravi, E.; Schrock, R. R.; Feast, W. J.; Gibson, V. C.; O'Regan, M. B.; Thomas, J. K.; Davis, W. M. *J. Am. Chem. Soc.* **1990**, *112*, 8378.
- (7) (a) Delaude, L.; Demonceau, A.; Noels, A. F. *Macromolecules* **1999**, *32*, 2091. (b) Delaude, L.; Demonceau, A.; Noels, A. F. *Macromolecules* **2003**, *36*, 1446. (c) Lee, J. C.; Parker, K. A.; Sampson, N. S. *J. Am. Chem. Soc.* **2006**, *128*, 4578. (d) Lin, W.-Y.; Wang, H.-W.; Liu, Z.-C.; Xu, J.; Chen, C.-W.; Yang, Y.-C.; Huang, S.-L.; Yang, H.-C.; Luh, T.-Y. *Chem. - Asian J.* **2007**, *2*, 764. (e) Song, A. R.; Lee, J. C.; Parker, K. A.; Sampson, N. S. *J. Am. Chem. Soc.* **2010**, *132*, 10513. (f) Leitgeb, A.; Wappel, J.; Slugovc, C. *Polymer* **2010**, *51*, 2927. (g) Kobayashi, S.; Pitet, L. M.; Hillmyer, M. A. *J. Am. Chem. Soc.* **2011**, *133*, 5794. (h) Zhang, J.; Matta, M. E.; Martinez, H.; Hillmyer, M. A. *Macromolecules* **2013**, *46*, 2535.
- (8) Straub, B. F. *Adv. Synth. Catal.* **2007**, *349*, 204.
- (9) Rosebrugh, L. R.; Marx, V. M.; Keitz, B. K.; Grubbs, R. H. *J. Am. Chem. Soc.* **2013**, *135*, 10032.
- (10) Keitz, B. K.; Fedorov, A.; Grubbs, R. H. *J. Am. Chem. Soc.* **2012**, *134*, 2040.
- (11) (a) Grutzner, J. B.; Jautelat, M.; Dence, J. B.; Smith, R. A.; Roberts, J. D. *J. Am. Chem. Soc.* **1970**, *92*, 7107. (b) Ivin, K. J.; Laverty, D. T.; Rooney, J. J. *Makromol. Chem.* **1977**, *178*, 1545.
- (12) In general, quantitative conversion of monomer to polymer was observed when using catalysts 1–6. Monodentate catalysts 7 and 8 were less active than their bidentate counterparts, however, giving 20–50% yield.
- (13) (a) Ivin, K. J.; Laverty, D. T.; Rooney, J. J. *Makromol. Chem.* **1978**, *179*, 253. (b) Ivin, K. J.; Laverty, D. T.; O'Donnell, J. H.; Rooney, J. J.; Stewart, C. D. *Makromol. Chem.* **1979**, *180*, 1989. (c) Gillan, E. M. D.; Hamilton, J. G.; Mackey, N. D.; Rooney, J. J. *J. Mol. Catal.* **1988**, *46*, 359.
- (14) Greene, R. M. E.; Hamilton, J. G.; Ivin, K. J.; Rooney, J. J. *Makromol. Chem.* **1986**, *187*, 619.
- (15) Amir-Ebrahimi, V.; Corry, D. A. K.; Hamilton, J. G.; Rooney, J. J. *J. Mol. Catal. A: Chem.* **1998**, *133*, 115.
- (16) (a) Davies, G. R.; Feast, W. J.; Gibson, V. C.; Hubbard, H. V. S. A.; Ivin, K. J.; Kenwright, A. M.; Khosravi, E.; Marshall, E. L.; Mitchell, J. P.; Ward, I. M.; Wilson, B. *Makromol. Chem., Macromol. Symp.* **1993**, *66*, 289. (b) McConville, D. H.; Wolf, J. R.; Schrock, R. R. *J. Am. Chem. Soc.* **1993**, *115*, 4413.
- (17) (a) Hamilton, J. G.; Ivin, K. J.; Rooney, J. J. *J. Mol. Catal.* **1985**, *28*, 255. (b) Feast, W. J.; Gibson, V. C.; Ivin, K. J.; Khosravi, E.; Kenwright, A. M.; Marshall, E. L.; Mitchell, J. P. *Makromol. Chem.* **1992**, *193*, 2103.
- (18) (a) Arnold, D. R.; Trecker, D. J.; Whipple, E. B. *J. Am. Chem. Soc.* **1965**, *87*, 2596. (b) Gilliom, L. R.; Grubbs, R. H. *J. Am. Chem. Soc.* **1986**, *108*, 733.
- (19) (a) Ivin, K. J.; Lapienis, G.; Rooney, J. J.; Stewart, C. D. *J. Mol. Catal.* **1980**, *8*, 203. (b) Ivin, K. J.; Laverty, D. T.; Reddy, B. S. R.; Rooney, J. J. *Makromol. Chem., Rapid Commun.* **1980**, *1*, 467.
- (20) Ho, H. T.; Ivin, K. J.; Rooney, J. J. *Makromol. Chem.* **1982**, *183*, 1629.
- (21) (a) Liu, P.; Xu, X.; Dong, X.; Keitz, B. K.; Herbert, M. H.; Grubbs, R. H.; Houk, K. N. *J. Am. Chem. Soc.* **2012**, *134*, 1464. (b) Dang, Y.; Wang, Z.-X.; Wang, X. *Organometallics* **2012**, *31*, 7222. (c) Dang, Y.; Wang, Z.-X.; Wang, X. *Organometallics* **2012**, *31*, 8654.
- (22) Hartung, J.; Grubbs, R. H. *J. Am. Chem. Soc.* **2013**, *135*, 10183.
- (23) (a) Khan, R. K. M.; Zhugralin, A. R.; Torker, S.; O'Brien, R. V.; Lombardi, P. J.; Hoveyda, A. H. *J. Am. Chem. Soc.* **2012**, *134*, 12438. (b) Torker, S.; Khan, R. K. M.; Hoveyda, A. H. *J. Am. Chem. Soc.* **2014**, *136*, 3439.

(24) For computational studies on ROMP with noncyclometalated ruthenium catalysts: (a) Song, A.; Chul-Lee, J.; Parker, K. A.; Sampson, N. S. *J. Am. Chem. Soc.* **2010**, *132*, 10513–10520.

(b) Martinez, H.; Miro, P.; Charbonneau, P.; Hillmyer, M. A.; Cramer, C. J. *ACS Catal.* **2012**, *2*, 2547.

(25) Frisch, M. J.; Trucks, G. W.; Schlegel, H. B.; Scuseria, G. E.; Robb, M. A.; Cheeseman, J. R.; Scalmani, G.; Barone, V.; Mennucci, B.; Petersson, G. A.; Nakatsuji, H.; Caricato, M.; Li, X.; Hratchian, H. P.; Izmaylov, A. F.; Bloino, J.; Zheng, G.; Sonnenberg, J. L.; Hada, M.; Ehara, M.; Toyota, K.; Fukuda, R.; Hasegawa, J.; Ishida, M.; Nakajima, T.; Honda, Y.; Kitao, O.; Nakai, H.; Vreven, T.; Montgomery, J. A., Jr.; Peralta, J. E.; Ogliaro, F.; Bearpark, M.; Heyd, J. J.; Brothers, E.; Kudin, K. N.; Staroverov, V. N.; Kobayashi, R.; Normand, J.; Raghavachari, K.; Rendell, A.; Burant, J. C.; Iyengar, S. S.; Tomasi, J.; Cossi, M.; Rega, N.; Millam, M. J.; Klene, M.; Knox, J. E.; Cross, J. B.; Bakken, V.; Adamo, C.; Jaramillo, J.; Gomperts, R.; Stratmann, R. E.; Yazyev, O.; Austin, A. J.; Cammi, R.; Pomelli, C.; Ochterski, J. W.; Martin, R. L.; Morokuma, K.; Zakrzewski, V. G.; Voth, G. A.; Salvador, P.; Dannenberg, J. J.; Dapprich, S.; Daniels, A. D.; Farkas, Ö.; Foresman, J. B.; Ortiz, J. V.; Cioslowski, J.; Fox, D. J. *Gaussian 09*, revision D.01; Gaussian, Inc.: Wallingford, CT, 2009.

(26) (a) Chen, P.; Adlhart, C. *J. Am. Chem. Soc.* **2004**, *126*, 3496.

(b) Naumov, S.; Buchmeiser, M. R. *J. Phys. Org. Chem.* **2008**, *21*, 963.